Received: 10 October 2016 | Revised: 11 January 2017 | Accepted: 17 January 2017

DOI 10.1002/jcp.25807

ORIGINAL ARTICLE

WILEY Journal of Cellular Physiology

Impact of lysosomal storage disorders on biology of mesenchymal stem cells: Evidences from in vitro silencing of glucocerebrosidase (GBA) and alpha-galactosidase A (GLA) enzymes

Tiziana Squillaro[1,2] | Ivana Antonucci[3] | Nicola Alessio[1] | Anna Esposito[1] | Marilena Cipollaro[1] | Mariarosa Anna Beatrice Melone[4] | Gianfranco Peluso[2] | Liborio Stuppia[3] | Umberto Galderisi[1]

[1] Department of Experimental Medicine, Biotechnology and Molecular Biology Section, University of Campania "Luigi Vanvitelli", Naples, Italy

[2] Institute of Bioscience and Bioresources, National Research Council, Naples, Italy

[3] Laboratory of Molecular Genetics, Department of Psychological, Health and Territorial Sciences, School of Medicine and Health Sciences, G. d'Annunzio University, Chieti-Pescara, Italy

[4] Department of Medical, Surgical, Neurological, Metabolic Sciences, and Aging; Division of Neurology and InterUniversity Center for Research in Neurosciences, University of Campania "Luigi Vanvitelli", Naples, Italy

Correspondence
Prof. Umberto Galderisi, Department of Experimental Medicine, Biotechnology and Molecular Biology Section, Second University of Naples, Via Costantinopoli 16, Napoli 80138, Italy.
Email: umberto.galderisi@unina2.it

Correspondence
Prof. Liborio Stuppia, Department of Psychological, Health and Territorial Sciences, School of Medicine and Health Sciences, G. d'Annunzio University, Chieti-Pescara, Via dei Vestini 31, 66013 Chieti, Italy.
Email: stuppia@unich.it

Lysosomal storage disorders (LDS) comprise a group of rare multisystemic diseases resulting from inherited gene mutations that impair lysosomal homeostasis. The most common LSDs, Gaucher disease (GD), and Fabry disease (FD) are caused by deficiencies in the lysosomal glucocerebrosidase (GBA) and alpha-galactosidase A (GLA) enzymes, respectively. Given the systemic nature of enzyme deficiency, we hypothesized that the stem cell compartment of GD and FD patients might be also affected. Among stem cells, mesenchymal stem cells (MSCs) are a commonly investigated population given their role in hematopoiesis and the homeostatic maintenance of many organs and tissues. Since the impairment of MSC functions could pose profound consequences on body physiology, we evaluated whether GBA and GLA silencing could affect the biology of MSCs isolated from bone marrow and amniotic fluid. Those cell populations were chosen given the former's key role in organ physiology and the latter's intriguing potential as an alternative stem cell model for human genetic disease. Our results revealed that GBA and GLA deficiencies prompted cell cycle arrest along with the impairment of autophagic flux and an increase of apoptotic and senescent cell percentages. Moreover, an increase in ataxia–telangiectasia-mutated staining 1 hr after oxidative stress induction and a return to basal level at 48 hr, along with persistent gamma-H2AX staining, indicated that MSCs properly activated DNA repair signaling, though some damages remained unrepaired. Our data therefore suggest that MSCs with reduced GBA or GLA activity are prone to apoptosis and senescence due to impaired autophagy and DNA repair capacity.

KEYWORDS
autophagy, fabry disease, gaucher disease, lysosomal storage disorders, mesenchymal stem cells, senescence

1 | INTRODUCTION

Lysosomal storage diseases (LSD) commonly refer to rare multisystemic disorders resulting from inherited gene mutations that impair lysosomal homeostasis. LSDs are characterized by deficiencies in lysosomal enzymes, which prompt the abnormal storage of macromolecular substrates (Platt, Boland, & van der Spoel, 2012). The most common inherited LSDs, Gaucher disease (GD) and Fabry disease (FD) are caused by deficiencies in the lysosomal glycosidases glucocerebrosidase (*GBA*) and alpha-galactosidase A (*GLA*), respectively.

Tiziana Squillaro and Antonucci Ivana contributed equally to the work.

On the one hand, GD is an autosomal recessive disorder with an annual incidence of about 1/60,000 in the general population (http://www.orpha.net/; (Ferraz et al., 2014; Nagral, 2014; Zion, Pappadopulos, Wajnrajch, & Rosenbaum, 2016). According to clinical features and the extent of central nervous system involvement, three types of GD have been classified. First, the most common type, GD1 (OMIM#230800), does not have neurological involvement and may occur at any age. Second, the acute neuronopathic form, GD2 (OMIM#230900), is usually fatal by 2 years of age. Third, the chronic neuronopathic form, GD3 (OMIM#231000), exhibits a later onset than GD2 (Nagral, 2014; Zion et al., 2016).

On the other hand, FD (OMIM#301500) is an X-linked disorder with an annual live-birth incidence of about 1/80,000. Usually appearing during childhood in male and female patients (http://www.orpha.net/; Ellaway, 2016; Hopkin et al., 2016), FD is associated with the dysfunction of many cell types and involves a systemic vasculopathy (Schiffmann, 2009).

Although cells and tissues of GD and FD patients show homogenous deficiency in lysosomal enzyme activity, the cell types presenting lysosomal accumulation of the glycosphingolipid substrates glucosylceramide and globotriaosylceramide, greatly differs between the two disorders, respectively (Ferraz et al., 2014). Therefore, the clinical manifestation of both disorders is entirely different. GD is characterized primarily by hepatosplenomegaly, bone marrow dysfunction, and skeletal disease, whereas FD patients show neurological, cutaneous, renal, cardiovascular, cochleovestibular, and cerebrovascular manifestations. To date, there is no cure for both diseases, although various treatments can help to control symptoms and prevent irreversible organ damage. Among them, enzyme replacement therapy is now the standard of care for patients with GD and FD. Although it can greatly modify or attenuate the phenotype, enzyme replacement therapy is lifelong and very expensive; moreover, side effects such as immune reactions against the infused enzyme and limitations such as the mistargeting of recombinant enzymes and difficult delivery to crucial tissues (i.e., brain and bone) have stressed the need for further research (Bailey, 2008; Nagral, 2014; Ortolano, Vieitez, Navarro, & Spuch, 2014). At present, the challenge for clinicians and researchers is to discover the safest, most effective therapeutic strategies to improve patients' quality of life.

Given the systemic nature of enzyme deficiency, the stem cell compartment of GD and FD patients can be also affected, which can pose profound consequences for an organism's physiology, since stem cells are responsible for maintaining tissue homeostasis and repairing subsequent injuries. Impairment of their functionality can induce defective tissue regeneration and aging, which in turn can have a deleterious effect on the entire organism (Behrens, van Deursen, Rudolph, & Schumacher, 2014).

Although several animal models of human genetic diseases (i.e., mice, rat, and zebrafish) are widely employed because of their high degree of sequence and functional homology with mammals, evidences produced by biomedical research in patient-derived cells provide highly informative insights (Guenet, 2011; Malafoglia, Bryant, Raffaeli, Giordano, & Bellipanni, 2013; Pinnapureddy et al., 2015). However, disease phenotypes are often restricted to specific cell types which could be difficult to isolate and cannot be expanded in vitro for several passages (Avior, Sagi, & Benvenisty, 2016). Thus, human stem cells can represent an interesting alternative for disease modeling given their intrinsic capability for self-renewal, high differentiation potential and the key role in physiology of an organism. Moreover, ectopic modulation of gene-disease in human stem cells is a versatile approach useful to mimic the effect due by its deregulation on cell biology.

Among stem cells, mesenchymal stem cells (MSCs) represent a very attractive source for disease modeling given their unique biological properties, including multilineage differentiation potential (i.e., bone, cartilage, and fat), ready availability from multiple tissues (i.e., bone marrow, adipose tissue, dental pulp, synovial membranes, amniotic fluid, Wharton's jelly), and extensive capacity for in vitro expansion (Fei et al., 2013; Gullo and De Bari, 2013; Heidari et al., 2013; Najar et al., 2010; Perry et al., 2008; Squillaro, Peluso, & Galderisi, 2016). In addition, MSCs play a key role in homeostatic maintenance of many organs and tissues. It is thus reasonable to hypothesize that the impairment of MSC function due to a systemic gene deficiency, as described for GD and FD, can have profound consequences on body physiology.

Recently, we demonstrated that in bone marrow MSCs (BMSCs), the alteration of lysosomal degradation of cellular molecules and components triggers senescence, a deleterious process for an organism ending in impairment of tissue renewal and function (Capasso et al., 2015). Given that a key feature of LSDs is the progressive accumulation of macromolecules within the cytoplasm due to impaired lysosomal degradation (Lieberman et al., 2012), we set up an in vitro model to evaluate the effects of *GBA* and *GLA* downregulation on MSC biology.

MSCs were isolated from bone marrow and amniotic fluid (AF). Our choices of those sources derived from the fact that BMSCs play a fundamental role in the physiology of organisms, while AFMSC represent a potential alternative novel source of stem cells for modeling human genetic diseases. In fact, by means of prenatal diagnosis, several fetuses affected by chromosomal or Mendelian diseases (such as GD and FD) can be identified, and amniotic fluid collected for genetic testing can be used after diagnosis to isolate AFMSCs. Those cells exhibit some features of pluripotency and an ability to differentiate in cells derived from all three germ layers in vitro, thereby representing a useful stem cell model for investigating the molecular basis of the diagnosed disease (Antonucci et al., 2016).

To determine whether mutations in *GBA* and *GLA* genes can induce an alteration of MSC biology, we silenced BMSCs and AFMSCs for the aforementioned genes and analyzed the cell cycle, autophagy, apoptosis, senescence, and DNA repair capacity. Ultimately, gene silencing represented a suitable in vitro model for mimicking GBA and GLA cellular deficiencies present in patients suffering from GD or FD. Indeed, mutations in GBA and GLA proteins reduced enzymatic activity like it occurs with the silencing of gene expression.

By extension, our research might provide new insights into dysfunctions associated with impaired *GBA* and *GLA* activities that lead to GD and FD, respectively. Moreover, a detailed understanding of cellular processes affected by *GBA* and *GLA* deficiency might prompt significant progress in the development of new therapies.

2 | MATERIALS AND METHODS

2.1 | BMSC cultures

Bone marrow samples were obtained from three healthy donors aged 6–10 years who provided their informed consent to participate. Cells were separated on Ficoll density gradient (GE Healthcare, Milan, Italy); successively, the mononuclear cell fraction was collected and washed in phosphate-buffered saline (PBS). We seeded $1.0–2.5 \times 10^5$ cells/cm^2 in α-minimum essential medium (α-MEM) containing 10% fetal bovine serum (FBS) and 2 ng/ml basic fibroblast growth factor (b-FGF). After 72 hr, non adherent cells were discarded while adherent cells were further cultivated for our experiments. In our experimental condition, MSC cultures fulfilled the minimal criteria for defining MSCs, as indicated by International Society for Cellular Therapy (ISCT), that are adherence to plastic, expression of specific surface antigen and multipotent differentiation capacity (Dominici et al., 2006). We evidenced that more than 90% of the plastic adherent MSCs expressed the CD105, CD73, and CD90 surface antigens. Finally, we verified that MSCs could differentiate into osteocytes, adipocytes, and chondrocytes. Cell culture reagents were purchased from Euroclone Life Sciences (Milan, Italy).

2.2 | AFMSC cultures

Amniotic fluid samples were obtained from two women receiving amniocentesis for prenatal diagnosis at 16–19 weeks of pregnancy and who provided their written informed consent to participate. This part of the study was approved by the Ethics Committee for Biomedical Research of G. d'Annunzio University in Chieti. For each sample, 2–3 ml of amniotic fluid, corresponding to a cell number ranging from 2×10^3 to 2×10^6 (Antonucci et al., 2012; Prusa & Hengstschlager, 2002), was centrifuged for 10 min at 1,800 rpm. Pellets were resuspended in Iscove's modified Dulbecco's medium supplemented with 20% FBS, 100 U/ml penicillin, 100 μg/ml streptomycin, 2 mM L-glutamine, and 5 ng/ml basic fibroblast growth factor, and incubated at 37°C with 5% humidified CO_2. Unselected AF-MSCs were immediately isolated from amniotic fluid and cultivated in media allowing their proliferation and rapid expansion. After 5 days, non adherent cells were removed and adherent ones allowed to grow in the same medium, which was changed every 2 days. When culture reached confluence (about 20 days after the primary culture), cells were treated with 0.05% trypsin and 0.02% ethylenediaminetetraacetic acid, counted, and replaced in 25-cm^2 culture flasks. Cell culture reagents were purchased from Euroclone Life Sciences.

2.3 | Gene silencing

siRNAs targeting the human *GBA* (β-glucosidase siRNA: sc-44904) and *GLA* (α-gal A siRNA: sc-105019) mRNA, as well as scrambled control siRNAs (control siRNA-A: sc-37007), were purchased from Santa Cruz Biotechnology (Santa Cruz, CA). BMSC and AFMSC cultures were transfected with siRNA GBA or siRNA GLA using Lipofectamine 2000 (Invitrogen, CA) according to the manufacturer's instructions. The efficiency of silencing was evaluated by quantitative reverse transcription polymerase chain reaction (RT-qPCR), as described below.

2.4 | RNA extraction and RT-qPCR

Total RNA was extracted from silenced and control MSCs using EuroGOLD Trifast (EuroClone Life Sciences) according to the manufacturer's instructions. mRNA expression levels of the interest genes were analyzed by RT-qPCR as previously reported (Alessio et al., 2010). Primer pairs for RT-qPCR reactions were designed using Primer Express software (Primer Express, Applied Biosystems). We used appropriate regions of GAPDH cDNA as internal controls, and each RT-qPCR reaction was repeated at least 3 times. Primer parameters and sequences are reported in Table 1.

2.5 | Cell cycle analysis

Silenced and control cells were collected and fixed in 70% ethanol and followed by PBS washes; subsequently, cells were resuspended in a hypotonic buffer containing propidium iodide. Samples were acquired on a Guava EasyCyte flow cytometer (Merck Millipore, Italy) and analyzed with a standard procedure using EasyCyte software.

2.6 | Cyto-ID® Autophagy Detection Kit

We used the Cyto-ID® Autophagy Detection Kit (Enzo Life Sciences, NY) to measure autophagic vacuoles and to monitor autophagic flux in live cells. The kit uses a cationic amphiphilic dye that selectively labels autophagic vacuoles. The percentage of positive cells was determined according to the manufacturer's instructions.

2.7 | Nexin V assay

The percentage of apoptotic cells were detected using a fluorescein conjugated annexin V kit (4500–0450 Guava Nexin Reagent, Merck Millipore). Sample were acquired on a Guava EasyCyte flow cytometer according to the manufacturer's instructions.

2.8 | In situ senescence-associated β-galactosidase assay

The percentage of blue β-alactosidase-positive cells (senescent cells) was calculated by counting at least 500 cells in different microscope fields, as previously reported (Debacq-Chainiaux, Erusalimsky, Campisi, & Toussaint, 2009).

2.9 | Immunocytochemistry for detecting ATM, gamma-H2AX, RAD51, and DNA-PK

The kinase ataxia–telangiectasia-mutated (ATM; ab36810, Abcam, UK), gamma-H2AX (2577, Cell Signaling, MA), RAD51 (ab88572, Abcam), and DNA-PK (sc390698, Santa Cruz Biotech) were detected according to the manufacturers' instuctions. Cell nuclei were stained with Hoechst 33342. Subsequently, cells were observed with a fluorescence microscope (Leica Italia, Italy). The percentage of

TABLE 1 Primer parameters and sequences

Gene	Primer position	Sequence	Annealing T (°C)	Melting T (°C)	Amplicon lenght (bp)
GAPDH (NM_002046.5)	121	5′-GGAGTCAACGGATTTGGTCGT-3′	58	80	161
	281	5′-ACGGTGCCATGGAATTTGC-3′			
GBA (NM_000157.3)	1307	5′-AATTGGGTGCGTAACTTT-3′	57	78	114
	1420	5′-CTCAGGAATGAACTTGCT-3′			
GLA (NM_000169.2)	833	5′-TATCTTGGACTGGACATC-3′	57	78	128
	960	5′-TCTGAGTTACTTGCTGAT-3′			
VEGFA (NM_001025366.2)	2111	5′-CAGTGCTAATGTTATTGGT-3′	57	79	110
	2220	5′-TCTCATCTCCTCCTCTTC-3′			
EGF (NM_001963.5)	1069	5′-CATTGGATGTGCTTGATAA-3′	56	76	126
	1194	5′-TATGCTGTGTTGGATGTT-3′			
HGF (NM_000601.5)	466	5′-TTCAATAGCATGTCAAGTG-3′	55	75	134
	599	5′-CTCTTAGTGATAGATACTGTTC-3′			
PDGFA (NM_002607.5)	501	5′-CAAGGTGGAATACGTCAG-3′	58	80	118
	618	5′-GTCCTCTTCCCGATAATC-3′			
IGF1 (NM_001111283.2)	432	5′-TTATTTCAACAAGCCCACA-3′	60	82	112
	543	5′-ATACATCTCCAGCCTCCT-3′			
IGFBP4 (NM_001552.2)	1494	5′-ATTCTGACTTCCTCTGATT-3′	56	77	102
	1595	5′-CTCTTCTCCTCTGACTCT-3′			
IGFBP5 (NM_000599.3)	5759	5′-AGATTCCGAGTTGCCTAC-3′	55	74	147
	5905	5′-AGAGAACAGAGTTATGGTATGA-3′			
IGFBP7 (NM_001553.2)	735	5′-TGGTATCTCCTCTAAGTAAG-3′	56	77	113
	847	5′-TTCATGTAAGGCATCAAC-3′			

ATM-, gamma-H2AX-, RAD51-, and DNA-PK-positive cells was calculated by counting at least 500 cells in different microscope fields.

2.10 | Western blotting

Silenced and control MSCs were lysed for 30 min at 4°C using a buffer containing 0.1%. From 10 to 40 µg of each lysate was processed by electrophoresis in a polyacrylamide gel and, then, transferred onto a nitrocellulose membrane. The primary antibodies β-Glucosidase (sc-365745 Santa Cruz Biotech) α-GAL-A (sc-25823, Santa Cruz Biotech), LC3 (ab51520, Abcam, Cambridge, UK), HPRT (sc-376938 Cruz Biotech, CA, USA); GAPDH (G8795, Sigma–Aldrich, MO); RB (9309, Cell Signaling, MA), RB2/P130 (610261 BD, NC), P107 (sc-318 Santa Cruz Biotech), P53 (sc-126 Santa Cruz Biotech), MDM2 (sc-965 Santa Cruz Biotech), P21 (sc-397 Santa Cruz Biotech), P27 (3686 Cell Signaling), and P16 (ab54210 Abcam), were used according to the manufacturers' instructions. Immunoreactive signals were detected using the ECL plus reagent (GE Healthcare), a chemiluminescent horseradish peroxidase substrate based system.

2.11 | Statistical analysis

Statistical analysis was carried out using one-way analysis of variance analysis followed by Student's *t* and Bonferroni's tests. Data with continuous outcomes were analyzed using mixed-model variance. GraphPad Prism statistical software package version 5.01 (GraphPad, CA) was used to analyzed all data.

3 | RESULTS

3.1 | BMSC and AFMSC silencing

Human BMSCs and AFMSCs were plated as described in the previous section. All experiments were conducted out on cultures at passage 3. Both cell cultures were tested for *GBA* and *GLA* knockdown after Lipofectamine transfection. BMSC-silenced for GBA or GLA genes were indicated as BMSC siGBA and siGLA, respectively. Analogously, AFMSC following silencing were indicated as AFMSC siGBA and siGLA. Control cells were silenced with a scrambled siRNA and were indicated as siCTRL.

GBA- and GLA-siRNAs were effective in silencing and decreasing target mRNAs for both cell cultures, as detected by RT-qPCR. In fact, we detected a roughly 85% decrease of *GBA* and *GLA* mRNAs in BMSCs and an 80% decrease in AFMSCs compared with respective control cells, as shown in Fig. 1A and B. The effect of silencing was further corroborated by analyzing the protein levels of GBA and GLA; as detected by WB analysis, we obtained a roughly 75% decrease of GBA and GLA protein in BMSCs and a 70% in AFMSCs compared to respective control cells (Fig. 1C and D).

3.2 | Impaired autophagy process due to GBA and GLA silencing

A key feature of LSDs is the progressive accumulation of macromolecules within the cytoplasm due to impaired lysosomal

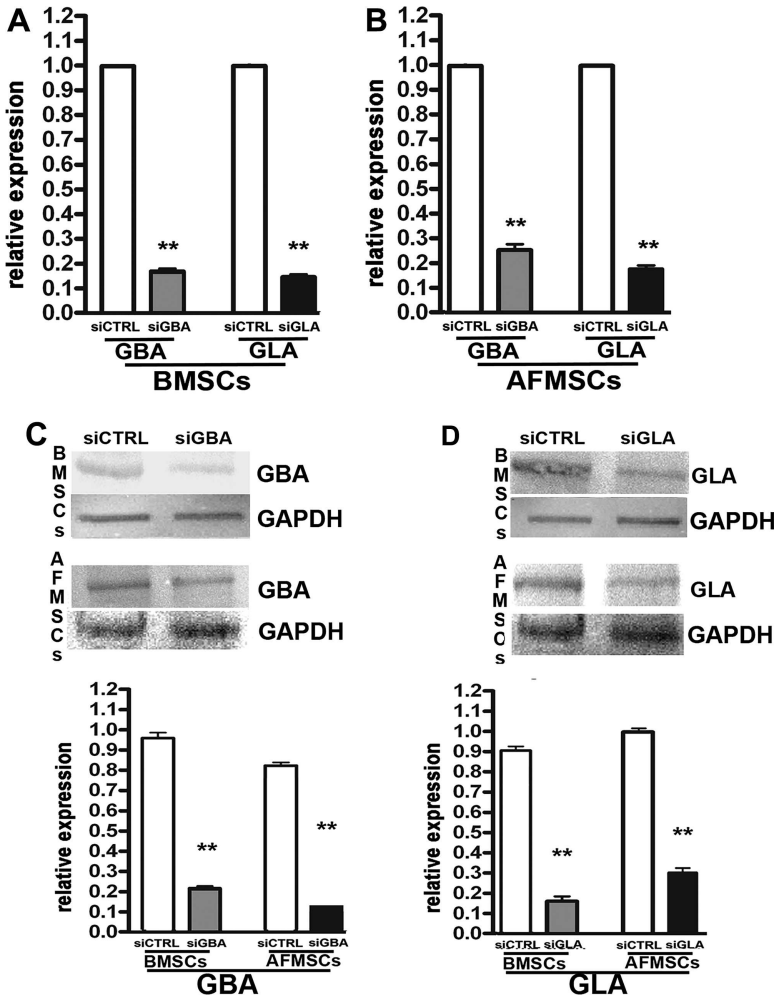

FIGURE 1 *GBA* and *GLA* silencing. (A and B) RT-qPCR analysis: mRNA levels were normalized with respect to GAPDH as the internal control. The histogram shows the mean expression values (±*SD*, $n = 3$). Changes in the mRNA levels of BMSC (A) and AFMSC (B) siGBA, and siGLA were compared with that of siCTRL cells as the reference ($^{*}p < 0.05$, $^{**}p < 0.01$). We used the comparative cycle threshold method to quantify expression levels. (C and D) Western blot analysis: representative western blots of GBA and GLA proteins (on the top); histograms show the mean expression values (on the bottom) (±*SD*, $n = 3$). Protein levels were normalized with respect to GAPDH as the internal control. Changes of GBA levels in BMSC and AFMSC siGBA (C), and changes of GLA levels in BMSC and AFMSC siGLA (D) were compared with those of siCTRL cells as a reference. ($^{**}p < 0.01$)

degradation. It has been repeatedly demonstrated that LSDs are accompanied by an ample spectrum of abnormalities in various cellular functions (Lieberman et al., 2012). Given the important role played by lysosomes in the autophagic pathway through fusion with autophagosomes and the digestion of their content, LSDs can principally be considered as autophagy disorders (Aflaki et al., 2016; Ballabio and Gieselmann, 2009; Lieberman et al., 2012). As such, we decided to investigate whether *GBA* and *GLA* silencing could determine impaired autophagy in BMSCs and AFMSCs, respectively.

To evaluate the autophagy process, the expression levels of LC3-I and LC3-II, two isoforms of the microtubule-associated protein 1 light chain 3 (LC3), a reliable marker of autophagosomes, were measured by western blotting. The autophagic flux were analyzed by tracking the conversion of LC3-I proteins to LC3-II. Following synthesis, LC3 is processed by mammalian Atg4s and appears in cytosol as LC3-I. When autophagy is induced, some LC3-I is converted into LC3-II, which is tightly bound to the autophagosome membrane (Alessio et al., 2015; Mizushima, 2004). The amount of LC3 at a certain time point does not indicate autophagic flux, and therefore, to determine changes in autophagic flux, it is important to measure the amount of LC3-II in both the presence and absence of lysosomal protease inhibitors (Alessio et al., 2015).

For that reason, following GBA and GLA silencing in BMSCs and AFMSCs, we determined the level of LC3 isoforms, both in the presence and absence of bafilomycin A1, an inhibitor of lysosomal degradation. *GBA* and *GLA* silencing induced a reduction of autophagic flux in both MSC cultures, thereby suggesting significant impairment of the autophagy process (Fig. 2A and B).

Impairment of autophagy was confirmed with the Cyto-ID® Autophagy Detection Kit, that measures autophagy with a cationic amphiphilic tracer dye that rapidly partitions into cells and enables the labeling of vacuoles associated with the autophagy pathway. The percentage of cells expressing active autophagic vacuoles was significantly decreased in both silenced cell cultures compared with the control ones (Fig. 2C and D).

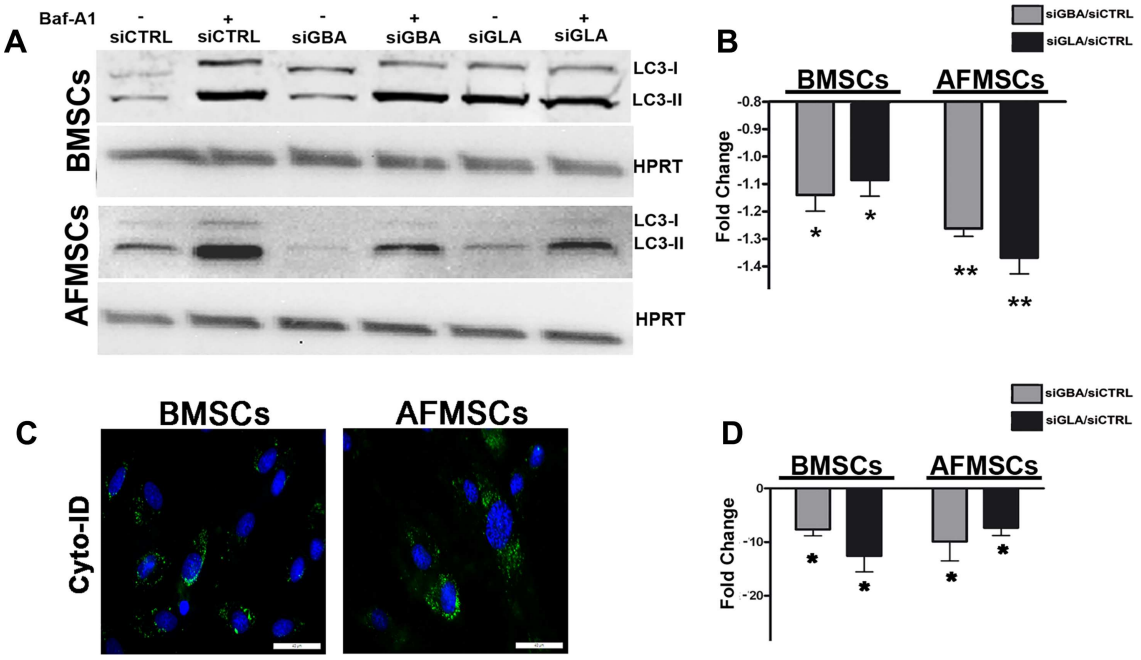

FIGURE 2 Autophagy detection assays. (A) show the detection of LC3-I and LC3-II in BMSC and AFMSC siGBA, siGLA, and siCTRL via western blot. Following silencing, cells were incubated for 48 hr and harvested for western blot analysis. For 2 hr before the end of cell sample preparation, silenced and control MSC cultures were incubated with 100 nM bafilomycin A1 as an inhibitor of lysosomal degradation or PBS to detect autophagic flux. We used Gel Doc 2000 Gel Documentation Systems (Bio-Rad Laboratories, Hercules, CA) to measure LC3-I and -II band intensities normalized with HPRT as the loading control. We determined the autophagic flux for LC3 II by using the following formulae: Autophagic flux of silenced MSCs = (Silenced MSCs + Bafilomycin A1) − (Silenced MSCs + PBS); Autophagic flux of control MSCs treated with siCTRL = (Control MSCs + Bafilomycin A1) − (Control MSCs + PBS). Change in autophagic flux (ΔAF) between silenced and control MSC was calculated as ΔAF = Autophagic flux of silenced MSCs − Autophagic flux of control MSCs. (B) The graphs show flux changes in siGBA and siGLA BMSCs and AFMSCs compared to respective control cultures. Data are expressed in fold change ($n = 3$; $^{*}p < 0.05$). (C and D) show the cyto-ID assay, particularly representative microscopic fields of cells with active autophagy (green) in silenced BMSCs and AFMSCs. Nuclei were counterstained with Hoechst 33342 (blue). Scale bar 40 μm,(C). The mean percentage value of positive cells is indicated in the graphs. Data are expressed in fold change (D) (±*SD*, $n = 3$, $^{*}p < 0.05$, $^{**}p < 0.01$)

These results prompted us to further investigate whether *GBA* and *GLA* silencing could affect key process regulating MSCs' biology, including cell cycle progression, apoptosis, senescence, and DNA repair capacity.

3.3 | Reduced percentage of S-phase cells and increased apoptosis due to GBA and GLA silencing

As determined by flow cytometry analysis, the downregulation of *GBA* and *GLA* genes modified the cell cycle profile of MSCs in the culture. In several experiments, we observed a significant reduction of S phase cells in both BMSC and AFMSC siGBA (5.5% vs. 10.1% and 7.6% vs. 12.3%, respectively), along with an increase of G1 cells in BMSC (79.5% vs. 68.0%) and of G2/M in AFMSC (16.1% vs. 9.0%) with respect to control cells (Fig. 3A and B). A similar trend was observed in both cell cultures following *GLA* silencing—briefly, a significant reduction of S phase cells in BMSCs and AFMSCs (4.5% vs. 10.1% and 7.7% vs. 12.3%, respectively). Analogously, an increase of G1 cells in BMSC (78.6% vs. 68.0%) and of G2/M in AFMSC (14.4% vs. 9.0%) with respect to control cells was clear, as Fig. 3A and B show.

Annexin V assay showed a statistically significant increase of apoptotic cells in BMSCs following *GBA* and *GLA* silencing compared with respective controls (5.3% vs. 3.4% and 6.5% vs. 3.4%, respectively), as Fig. 4A and B illustrates. Those figures also reveal an increased percentage of apoptotic cells in AFMSC siGBA and siGLA (7.5% vs. 3.7% and 8.2% vs. 3.7%, respectively).

3.4 | Promotion of senescence due to GBA and GLA silencing

Since our findings demonstrated that *GBA* and *GLA* silencing affected cell cycle progression and apoptosis in BMSCs and AFMSCs, we investigated whether it could also affect senescence.

Senescent cells were detected via acid β-galactosidase assay in BMSCs and AFMSCs following *GBA* and *GLA* silencing. Although β-galactosidase positive cells showing characteristic senescent morphology (i.e., flat, enlarged cells) emerged in both cell cultures, a remarkable increase in percentage of senescent cells was observed in BMSCs silenced for the *GBA* and *GLA* gene (40% vs. 16% and 50% vs. 16%, respectively), as Fig. 4C and D show. Those figures also illustrate that in AFMSC siGBA, and siGLA, the percentage of β-galactosidase positive cells was 22.8% versus 12.2% and 18.4% versus 12.2%, respectively.

To extend those findings, we used RT-qPCR to analyze the expression levels of several cellular growth factors, including *VEGFA*, *EGF*, *HGF*, *PDGFA*, and *IGF1*, involved in cellular growth and

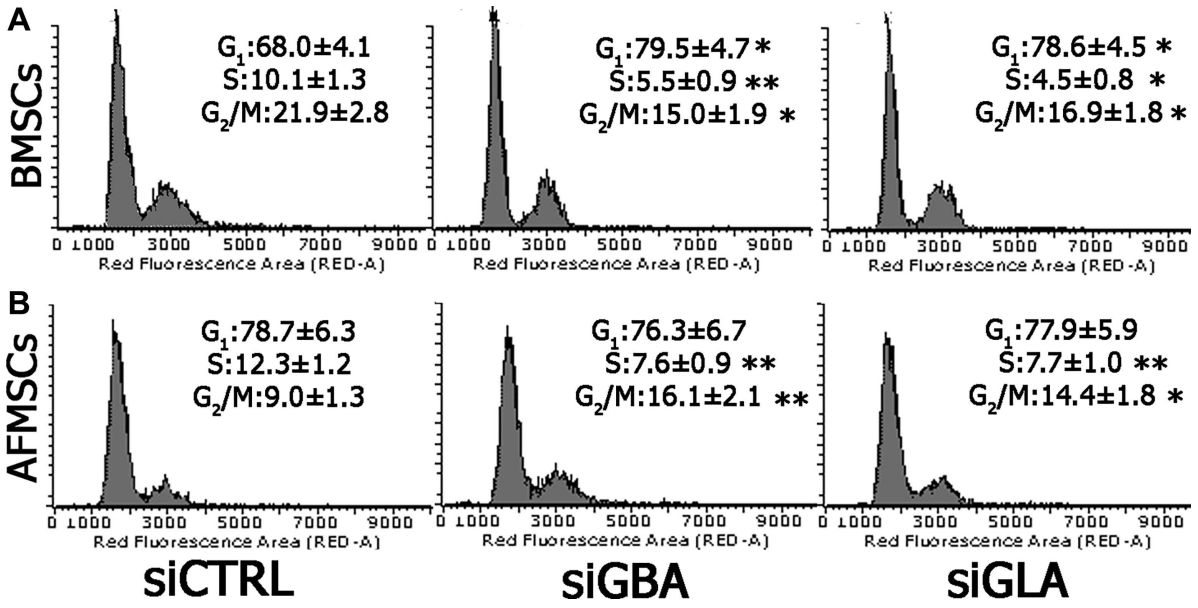

FIGURE 3 Cell cycle analysis. (A and B) show representative FACS analysis of BMSC (on the top) and AFMSC (on the bottom) siGBA, siGLA, and siCTRL, respectively. Experiments were conducted in triplicate. The graphs indicate the percentage of different cell populations (G1, S, and G2/M). Data are expressed with *SD* ($n = 3$, $^{*}p < 0.05$, $^{**}p < 0.01$)

proliferation. Those factors were secreted by healthy MSCs and showed an expression negatively affected by senescence (Galderisi and Giordano, 2014; Ozcan et al., 2016; Severino et al., 2013). A significant decrease in the expression of *EGF*, *HGF*, and *IGF1* occurred in BMSCs following *GBA* and *GLA* silencing in respect to control cells (Fig. 5A). On the contrary, a significant increase in *VEGFA* and *PDGFA* mRNA levels was observed in AFMSC siGLA and siGBA (Fig. 5B). We also evaluated the mRNA expression levels of *IGFBP4*, *IGFBP5*, and *IGFBP7*, all of which are considered to be key components needed to trigger senescence in young MSCs. Our previous results showed that conditioned media of senescent MSCs contain a set of secreted factors (i.e., *IGFBP4* and *IGFBP7*) that can induce full senescence in young cells (Severino et al., 2013). In the current experiment, a significant increase in expression for all genes occurred in BMSC siGBA and siGLA with respect to control cells (Fig. 5C). Conversely, a decrease in *IGFBP4* and *IGFBP5* mRNA levels was observed in AFMSCs following *GBA* and *GLA* silencing (Fig. 5D).

3.5 | Impaired DNA repair system due to GBA and GLA silencing

DNA damage-sensing and -signaling pathways, commonly referred to as the *DNA damage response network*, are related to cellular senescence and apoptosis (Lombard et al., 2005; Roos & Kaina, 2006). The activation of the cell cycle checkpoint and repair mechanisms represents the cell response to DNA damage, which, when irreparable, can cause damaged cells to be eliminated either by apoptosis or senescence.

The aforementioned changes in apoptosis and senescence rates in both BMSCs and AFMSCs with silenced *GBA* and *GLA* proteins prompted us to investigate the degree of DNA damage and the activation of DNA damage repair (DDR) pathway in our cell system. Moreover, to further examine if *GBA* and *GLA* silencing may render MSCs more or less sensitive to DNA damage we treated these cells with H_2O_2, a known DNA damaging agent (D'Errico, Parlanti, & Dogliotti, 2008). The choice of these stressor agents derives from the consideration that cells are exposed to reactive oxygen species deriving from cell metabolism. Given that, following genotoxic stress, the activation of DDR pathway occurs during short period of time and may persist for some hours, we carried out all the DDR analyses at basal conditions and, 1 and 48 hr post H_2O_2 treatment (Alessio et al., 2015).

The activation of the DNA repair system was evaluated by analyzing ATM kinase, which regulates DNA repair. Activation of ATM by autophosphorylation on Ser1981 occurs in response to exposed DNA double strand breaks (Alessio et al., 2015; Lee and Paull, 2007). Since ATM and its downstream effectors signal in pulses, after binding to DNA damaged foci, ATM dephosphorylates and dissociates from the foci (Alessio et al., 2015; Freeman & Monteiro, 2010).

Although silencing increased ATM-positive cells in basal conditions in both MSC cultures, the phenomenon was more remarkable in BMSC siGLA and AFMSC siGBA and siGLA than in the control culture (Fig. 6A–D). Following H_2O_2 treatment for 1 hr, the percentage of ATM-positive cells even increased, but did not reach levels observed in control cells, except in BMSC siGLA. After 48 hr following H_2O_2 administration, the number of positive cells decreased and, except for BMSC siGBA, reached levels lower than those observed in respective control cells (Fig. 6A–D).

We also evaluated the expression of RAD51 and DNA-PK, which play a key role in activating homologous and non homologous end-joining (NHEJ) DNA repair systems, respectively (Polo & Jackson, 2011; Shibata et al., 2011). As noted for ATM detection, we also observed an increased number of RAD51-positive cells in the basal conditions in both silenced cell cultures in respect to control ones.

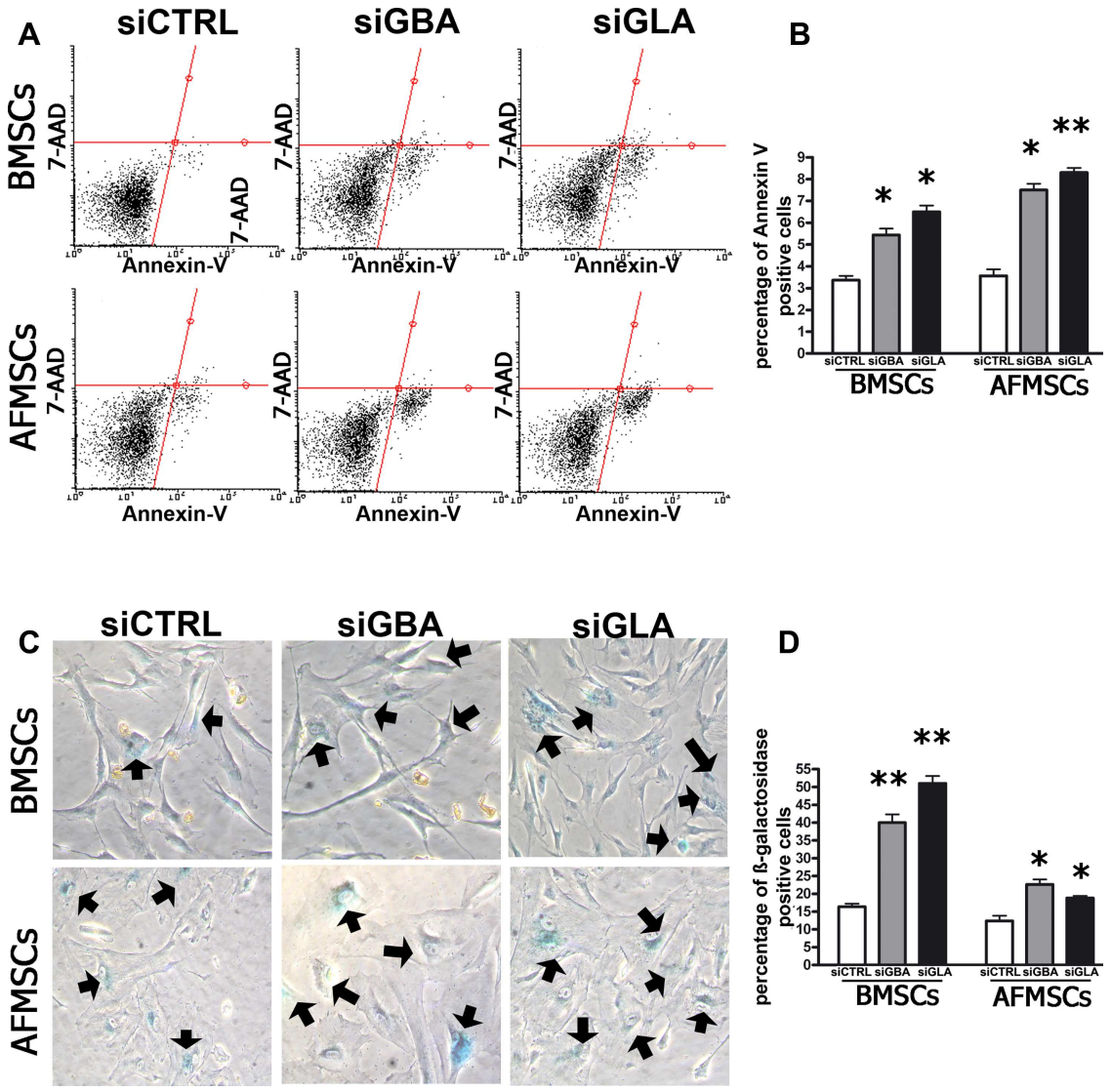

FIGURE 4 Analysis of apoptosis and senescence in BMSC and AFMSC siGBA, siGLA, and siCTRL. (A) depicts the flow cytometry analysis of apoptosis with nexin assay. The experiments were performed 48 hr after silencing. The assay allows the identification of early (annexin V+ and 7ADD-) and late apoptosis (annexin V+ and 7ADD+). Given that apoptosis is a continuous process we calculated the percentage of apoptosis as the sum of early and late apoptotic cells in order to avoid any discretional separation between early and late apoptosis. The histogram in (B) shows the global percentage of annexin V-positive cells (±*SD*, $n = 3$, $^{*}p < 0.05$; $^{**}p < 0.01$). (C) shows the senescence assay. Representative microscopic fields of acid β-galactosidase (blue) in silenced and control BMSCs and AFMSCs are shown. Arrows indicate senescent cells. The histogram in (D) shows the mean percentage value of senescent cells (±*SD*, $n = 3$, $^{*}p < 0.05$, $^{**}p < 0.01$)

After 1 hr following H_2O_2 treatment, we detected a significant increase in the number of RAD51 positive cells for both silenced cell cultures in respect to that of control cells (Fig. 6E–H). After treatment for 48 hr, the percentage of RAD51-positive cells decreased until reaching the level observed in control cultures. Interestingly, we evidenced a decrease of RAD51-positive cells in silenced cells following H_2O_2 treatment for 1 hr compared to treated control cultures (Fig. 6E–H).

Although the same trend was detected for DNAPK as well, we noticed an increase of DNAPK-positive cells exclusively in silenced BMSCs treated for 1 hr when compared to treated control cells (Fig. 6I–L).

Altogether, our findings strongly suggest that the DNA repair system was properly activated following *GBA* and *GLA* silencing and oxidative stress induction. Furthermore, our data indicate that silenced BMSCs following H_2O_2 treatment respond to DNA damage by preferentially activating NHEJ DNA repair systems.

The histone H2AX is an important downstream target of ATM; indeed, following the activation of ATM it is rapidly phosphorylated. The phosphorylated H2AX (gamma-H2AX) is involved in the recruitment or retaining of DNA repair and checkpoint proteins. Gamma-H2AX foci signals damaged DNA undergoing the repair process, and the persistence of the foci for hours or days following genotoxic stress indicates the presence of unrepaired DNA in cells' nuclei (Alessio et al., 2015; Fu et al., 2012; Kao et al., 2006).

Both BMSC and AFMSC silenced with siGBA and siGLA showed a significant augmentation of cells with a high number of gamma-H2AX foci after 1 hr that persisted even 48 hr after H_2O_2 administration

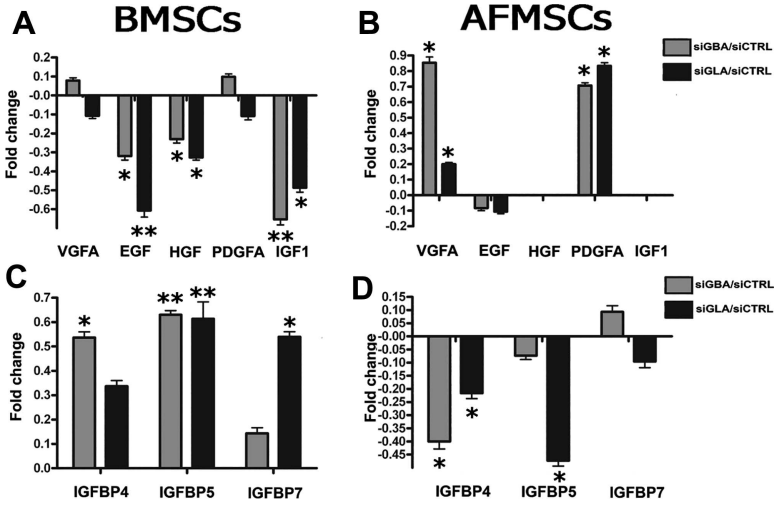

FIGURE 5 Gene expression analysis. RT–qPCR of indicated mRNAs in silenced BMSCs (A and C) and AFMSCs (B and D). mRNA levels were normalized in regard to GAPDH as an internal control. The histogram shows the mean expression values (±*SD*, $n = 3$). Changes in the mRNA levels of BMSC and AFMSC siGBA and siGLA were compared with those of siCTRL cells as a reference. Data are expressed in fold change (*$p < 0.05$, **$p < 0.01$). We used the comparative cycle threshold method to quantify expression levels

(Fig. 7A–D). This result suggests that despite DNA repair system activation, it could not entirely repair the damages.

3.6 | Molecular pathways involved in cell cycle regulation, apoptosis, and senescence: RB and P53 crosstalk

RB and *P53* are master genes that control cell cycle arrest, differentiation, DNA repair, apoptosis, senescence, and cellular stress responses (Campisi and d'Adda, 2007; Felsani, Mileo, & Paggi, 2006; Galderisi, Cipollaro, & Giordano, 2006; Oberdoerffer and Sinclair, 2007; Rufini, Tucci, Celardo, & Melino, 2013). RB and other retinoblastoma family proteins (RB2/P130 and P107) are critical in the progression and control of the cell cycle, specifically in the progression from the G_0 to S phases (Galderisi et al., 2006; Sun, Bagella, Tutton, Romano, & Giordano, 2007). In recent years, the role of RB family proteins as critical effectors of cellular senescence has also been described (Alessio et al., 2013; Fiorentino, Symonds, Macaluso, & Giordano, 2009; Kapic et al., 2006; Narita et al., 2003).

As a key guardian of the genome, P53 prevents the propagation of abnormal cells at risk of becoming cancer cells (Zuckerman, Wolyniec, Sionov, Haupt, & Haupt, 2009). Indeed, acting largely as a transcription factor, it can trigger various antiproliferative programs by activating or repressing key effector genes (Zilfou & Lowe, 2009). As such, we sought to evaluate in both MSC cultures whether the biological effects of *GBA* and *GLA* silencing were regulated by RB and P53 pathways.

Following *GBA* and *GLA* silencing, we observed no modification of RB protein levels in AFMSCs and a decrease in BMSCs in respect to control cultures. Conversely, the expression levels of RB2/P130 and P107 were strongly upregulated in both silenced cell cultures (Fig. 8A–D). We did not observe any significant changes in P53 protein levels in BMSC siGBA and siGLA, whereas a strong upregulation occurred in AFMSC following the silencing of both genes. We also evaluated the expression level of MDM2, the principal cellular antagonist of the *P53* gene. Several studies have suggested that MDM2 promotes P53 degradation (Shi & Gu, 2012). After silencing, however, we found no evidence of any significant modification of MDM2 expression levels in either cell culture (Fig. 8A–D).

It has been widely demonstrated that some cyclin kinase inhibitors such as $P21^{CIP1}$, $P27^{KIP1}$, and $P16^{INK4A}$ show pathways that overlap with the RB family and P53 (Alessio et al., 2015). Indeed, their activation and inactivation play a role in determining whether cells undergo senescence or apoptosis (Galderisi et al., 2006; Zuckerman et al., 2009). In particular, $P21^{CIP1}$ and $P16^{INK4A}$ are often expressed in senescent cells (Campisi & d'Adda, 2007). After in vitro silencing of GBA and GLA genes, we did not observe any significant changes in the expression of $P21^{CIP1}$ or $P27^{KIP1}$. However, a significant increase in $P16^{INK4A}$ occurred, albeit exclusively in silenced BMSCs, compared to control cells (Fig. 8A–D). Such results suggest that following *GBA* and *GLA* silencing, cell cycle arrest and senescence can occur via RB2/p130-$P16^{INK4A}$ and RB2/p130-P53 pathways in BMSCs and AFMSCs, respectively.

4 | DISCUSSION

The most common inherited LSDs, GD, and FD are caused by mutations in the lysosomal glycosidases *GBA* and *GLA*, respectively. Deficient lysosomal activity induces a progressive accumulation of storage materials within lysosomes, which ultimately precipitates organ dysfunctions (Ortolano et al., 2014).

Given the systemic nature of enzyme deficiency, we hypothesized that the stem cell compartment of GD and FD patients might be also affected. We therefore evaluated the effects of *GBA* and *GLA* silencing on the biology of MSCs isolated from bone marrow and amniotic fluid.

These cell populations were chosen given the former's key role in organ physiology and the latter's intriguing potential as alternative stem cell model for human genetic disease.

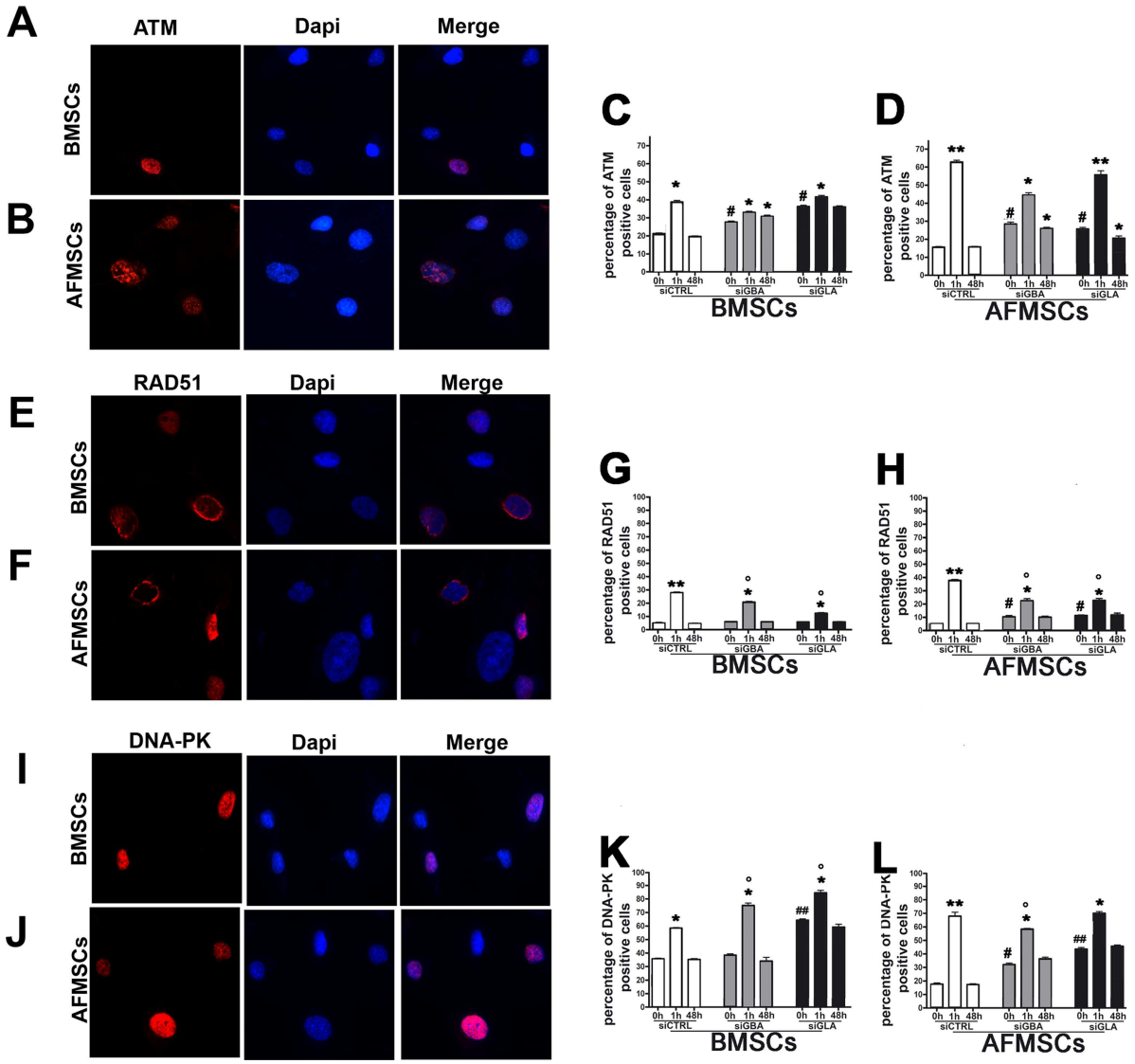

FIGURE 6 Evaluation of DNA damage and repair in BMSC and AFMSC siGBA, siGLA, and siCTRL following H_2O_2 treatment for 1 and 48 hr. (A and B) show representative fluorescence photomicrographs illustrating the merging of BMSC (on the top) and AFMSC (on the bottom) stained with anti-ATM (red) and Dapi (blue). (C and D) show the mean percentage of ATM positive cells in the graph, whereas (E and F) show representative fluorescence photomicrographs illustrating the merging of BMSC (on the top) and AFMSC (on the bottom) stained with anti-RAD51 (red) and Dapi (blue). (G and H) show the mean percentage of RAD51-positive cells in the graph, and (I and J) show representative fluorescence photomicrographs illustrating the merging of BMSC (on the top) and AFMSC (on the bottom) stained with anti-DNA-PK (red) and Dapi (blue). (K and L) show the mean percentage of DNA-PK-positive cells in the graph (±*SD*, $n = 3$, $^{*}p < 0.05$; $^{**}p < 0.01$ for 1 or 48 hr vs. 0 hr in each experimental group; intergroup comparison: $^{\#}p < 0.05$; $^{\#\#}p < 0.01$ refers to siGBA 0 hr or siGLA 0 hr vs. siCTRL 0 hr; °<0.05 siGBA 1 hr or siGLA 1 hr vs. siCTRL 1 hr)

As expected, following *GBA* and *GLA* silencing, an impairment of autophagic flux was observed in both cell types. Indeed, our data stressed the fundamental role played by lysosomes in the autophagic pathway (Lieberman et al., 2012) and thus support the suitability of these cells as in vitro models for studying GD and FD.

Consequently, we evaluated whether *GBA* and *GLA* silencing could affect MSC biology. In both cell cultures, siGBA and siGLA showed a significant reduction of S-phase cells, along with an increase of G_1 cells in BMSCs and of G_2/M in AFMSCs compared with control cells (Fig. 3A and B). We hypothesize that the differences in cell cycle arrest we observed might be due to the activation of different DNA repair systems (NHEJ or HR) in the two stem cell populations. Indeed, NHEJ is more associated with G_1 arrest while HR may occur only during replication and post-replication phases (Mao, Bozzella, Seluanov, & Gorbunova, 2008).

These results are in line with findings observed in MSCs from an LDS patient demonstrating impaired growth potential and cell cycle abnormalities (Lecourt et al., 2013).

Consistent with data indicating that cells from human patients suffering from GD and FD are more susceptible to apoptosis (De Francesco, Mucci, Ceci, Fossati, & Rozenfeld, 2011; Wei et al., 2008; Yoo & Kim, 2015), we demonstrated that *GBA* and *GLA* deficiency determined a significantly increased percentage of apoptotic cells in both stem cell cultures (Fig. 4A). Notably, although signs of senescence

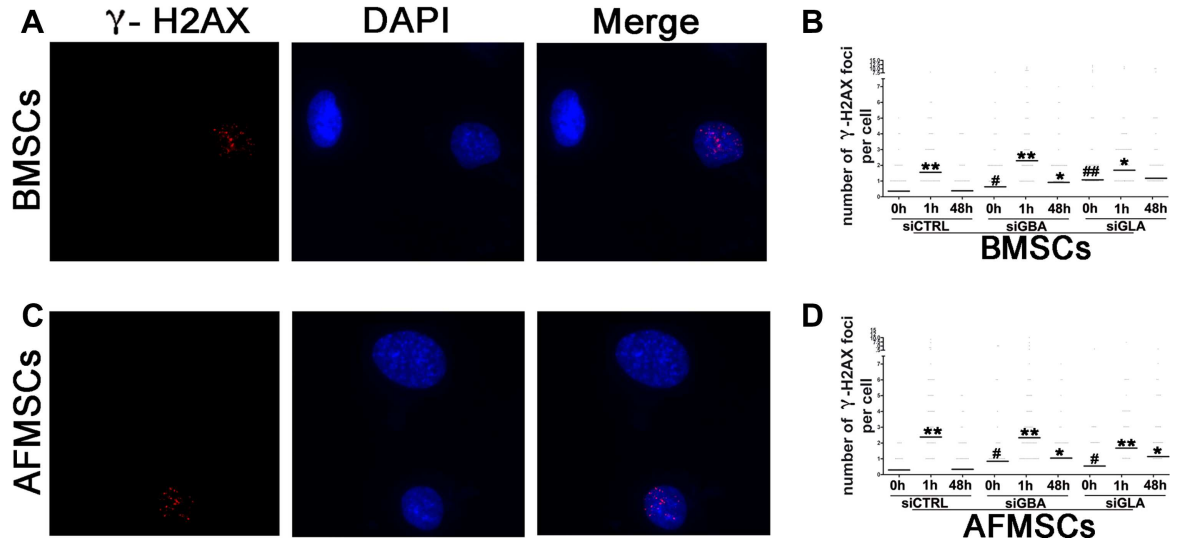

FIGURE 7 Gamma H2AX staining. (A and C) show representative fluorescence photomicrographs illustrating the merging of BMSC (on the top) and AFMSC (on the bottom) stained with anti-H2AX (red) and Dapi (blue). (B and D) show a graph depicting the degree of H2AX phosphorylation in BMSC (on the top) and AFMSC (on the bottom) siGBA, siGLA, and siCTRL following H_2O_2 treatment for 1 and 48 hr, evaluated by counting the number of gamma-H2AX immunofluorescent foci per cell. Foci number was determined for 200 cells, and each dot represents an individual cell. Black bars indicate mean value for each category (±*SD*, $n = 3$, $^{*}p < 0.05$; $^{**}p < 0.01$ refers to 1 or 48 hr vs. 0 hr within each experimental group; intergroup comparison: $^{\#}p < .05$; $^{\#\#}p < 0.01$ refers to siGBA 0 hr or siGLA 0 hr versus siCTRL 0 hr)

were observed in both silenced cell types, as detected by in situ acid β-galactosidase staining, a remarkably increased percentage of senescent cells appeared primarily in silenced BMSC in respect to control cells (Fig. 4B).

Senescence induction in silenced BMSCs was confirmed by decreased mRNA expression of cellular growth factors *EGF*, *HGF*, and *IGF1*, along with an increase of *IGFBP4*, *IGFBP5*, and *IGFBP7*, which are considered to be crucial components for triggering senescence in young MSCs (Severino et al., 2013). Our findings concerning senescence induction following *GBA* and *GLA* silencing in both cell cultures match results regarding impaired autophagy. A complex relationship between senescence and autophagy has been widely

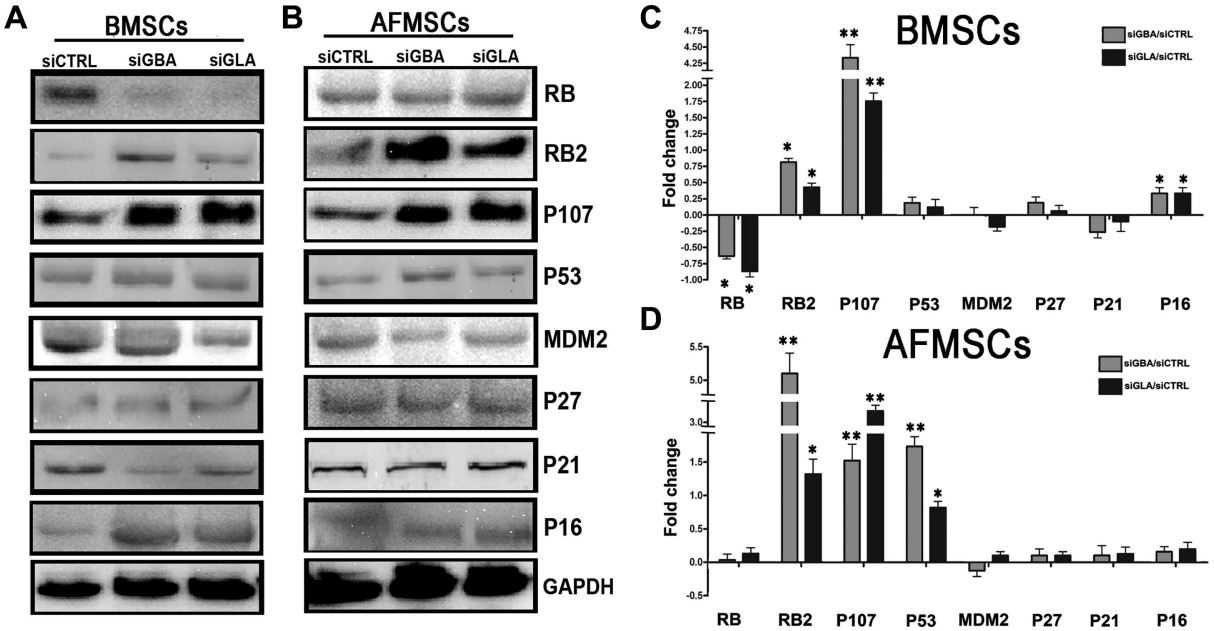

FIGURE 8 Gene expression analysis of RB- and P53-related pathways in BMSC and AFMSC siGBA and siGLA. (A and B) show a representative western blot of indicated proteins in BMSC and AFMSC siCTRL, siGBA, and siGLA. Proteins levels were normalized with GAPDH as an internal control. (C and D) depict histograms showing mean expression values (±*SD*, $n = 3$). Changes in the protein levels of BMSC and AFMSC siGBA and siGLA were compared with those of siCTRL cells as a reference. Data are expressed in fold change ($^{*}p < 0.05$, $^{**}p < 0.01$)

demonstrated, although evidence of opposite outcomes fuel debate on the issue. In some cases, the induction of senescence depends on a prior induction of autophagy, whereas several other studies have shown that impaired autophagy promotes senescence.

Our results supported the latter hypothesis since *GBA* and *GLA* silencing determined an impaired autophagy process, which in turn seemed to trigger senescence in MSCs. Moreover, our data are consistent with those of studies demonstrating that the inhibition of the mTOR pathway, whose activity is required for inducing senescence, promotes autophagy and rescues cells from the senescence process (Blagosklonny, 2012; Leontieva & Blagosklonny, 2010; Schug, 2010; Xu, Cai, & Wei, 2014).

Changes in senescence and apoptosis rates in silenced BMSCs and AFMSCs prompted us to investigate the degree of DNA damage and the activation of the DDR pathway in both basal conditions and following oxidative stress induction. The increase in ATM staining 1 hr after H_2O_2 treatment and its drop to basal levels at 48 hr, along with lasting gamma-H2AX staining, suggested that silenced BMSCs and AFMSCs properly activated the DNA repair signaling system, although some damages remained unrepaired. Indeed, ATM and its downstream effectors signal in pulses that arise from periodic examinations of the status of DNA damage. ATM activity is finely regulated to avoid the activation of the DNA damage response in the absence of damage, as well as to allow rapid cessation of the signal once DNA damage sites have been recognized, regardless of whether they have been properly repaired. At the same time, gamma-H2AX can remain bound to unrepaired DNA, as suggested by kinetics analysis of gamma-H2AX clearance due to DNA-damaging agents (Alessio et al., 2015, 2016; Fu et al., 2012; Kao et al., 2006). Rodier and Campisi (2011) demonstrated evidence that persistent unrepaired DNA foci can trigger senescence by showing that persistent foci of damaged DNA, termed *DNA-SCARS*, sustain damage-induced senescence growth arrest. Consistent with our data, another recent study reported that even if DNA repair is induced in FD patients, such repair cannot reduce DNA damage to control levels (Biancini et al., 2015).

Immunocytochemistry experiments for DNAPK and RAD51 detection suggested that the impaired DNA repair capacity of silenced BMSCs following H_2O_2 treatment seemed to primarily relate to the reduced activity of the NHEJ system. Indeed, silenced BMSCs respond to DNA damage by preferentially activating NHEJ DNA repair systems instead of homologous ones. That dynamic might suggest that even if the NHEJ mechanism were activated following DNA injury, it would be unable to properly repair the DNA.

We analyzed the expression of genes belonging to P53- and RB-associated pathways to further clarify the molecular pathways associated with impaired biological processes in silenced MSCs (Campisi & d'Adda, 2007; Galderisi et al., 2006; Oberdoerffer & Sinclair, 2007). Western blot experiments showed that senescence or apoptosis, if not both, relies on the activation of RB2/P130-$P16^{INK4A}$ or RB2/P130-P53 pathways in silenced BMSCs and AFMSCs, respectively. Such data are consistent with findings showing that retinoblastoma proteins, P53 and cyclin kinase inhibitors rank among the chief regulators of the cell cycle, cell apoptosis, and cell senescence (Campisi & d'Adda, 2007; Galderisi et al., 2006, 2009; Helmbold, Komm, Deppert, & Bohn, 2009; Kapic et al., 2006; Odell, Askham, Whibley, & Hollstein, 2010; Rayess, Wang, & Srivatsan, 2012).

Altogether, our data suggest that the chief consequence of *GBA* and *GLA* downregulation in BMSCs and AFMSCs triggers apoptosis or senescence, if not both.

5 | CONCLUSIONS

Our data suggest that BMSCs and AFMSCs with reduced *GBA* or *GLA* activity are prone to apoptosis and senescence due to impaired autophagy and DNA repair capacity. By extension, our results pave the way for further analysis, given that the senescence of the MSC compartment could profoundly affect tissue and organ physiology in GD and FD patients. It would, therefore, be worthwhile to determine whether anti-senescence treatments (e.g., mTOR inhibition) can ameliorate patients' symptoms or decelerate the progression of the diseases, if not both.

Our study demonstrated that AFMSCs can represent a novel source of stem cells for modeling human genetic diseases and supported that they could become a primary experimental model in the near future. Notably, AFMSCs obtained from fetuses affected by genetic diseases might be an appropriate alternative to animal experimentation, since they overcome all limitations related to preclinical research, including the ethical dilemmas and excessive costs inherent in animal models (Antonucci et al., 2016).

ACKNOWLEDGEMENTS

The research leading to these results has received funding from the Sanofi-Aventis S.p.A Unità locale di Modena, Modena, Italy.

REFERENCES

Aflaki, E., Moaven, N., Borger, D. K., Lopez, G., Westbroek, W., Chae, J. J., ... Sidransky, E. (2016). Lysosomal storage and impaired autophagy lead to inflammasome activation in Gaucher macrophages. *Aging Cell*, *15*(1), 77–88.

Alessio, N., Bohn, W., Rauchberger, V., Rizzolio, F., Cipollaro, M., Rosemann, M., ... Galderisi, U. (2013). Silencing of RB1 but not of RB2/P130 induces cellular senescence and impairs the differentiation potential of human mesenchymal stem cells. *Cellular and Molecular Life Sciences: CMLS*, *70*(9), 1637–1651.

Alessio, N., Capasso, S., Di Bernardo, G., Cappabianca, S., Casale, F., Calarco, A., ... Galderisi, U. (2016). Mesenchymal stromal cells having inactivated RB1 survive following low irradiation and accumulate damaged DNA: Hints for side effects following radiotherapy. *Cell Cycle*, 0. [Epub ahead of print]

Alessio, N., Del Gaudio, S., Capasso, S., Di Bernardo, G., Cappabianca, S., Cipollaro, M., ... Galderisi, U. (2015). Low dose radiation induced senescence of human mesenchymal stromal cells and impaired the autophagy process. *Oncotarget*, *6*(10), 8155–8166.

Alessio, N., Squillaro, T., Cipollaro, M., Bagella, L., Giordano, A., & Galderisi, U. (2010). The BRG1 ATPase of chromatin remodeling complexes is involved in modulation of mesenchymal stem cell senescence through RB-P53 pathways. *Oncogene*, *29*(40), 5452–5463.

Antonucci, I., Pantalone, A., Tete, S., Salini, V., Borlongan, C. V., Hess, D., & Stuppia, L. (2012). Amniotic fluid stem cells: A promising therapeutic resource for cell-based regenerative therapy. *Current Pharmaceutical Design*, *18*(13), 1846–1863.

Antonucci, I., Provenzano, M., Rodrigues, M., Pantalone, A., Salini, V., Ballerini, P., ... Stuppia, L. (2016). Amniotic fluid stem cells: A novel source for modeling of human genetic diseases. *International Journal of Molecular Sciences*, *17*(4). [Epub ahead of print]

Avior, Y., Sagi, I., & Benvenisty, N. (2016). Pluripotent stem cells in disease modelling and drug discovery. *Nature Reviews Molecular Cell Biology*, *17*(3), 170–182.

Bailey, L. (2008). An overview of enzyme replacement therapy for lysosomal storage diseases. *OJIN*, *13*(1), 3.

Ballabio, A., & Gieselmann, V. (2009). Lysosomal disorders: From storage to cellular damage. *Biochimica et Biophysica Acta*, *1793*(4), 684–696.

Behrens, A., van Deursen, J. M., Rudolph, K. L., & Schumacher, B. (2014). Impact of genomic damage and ageing on stem cell function. *Nature Cell Biology*, *16*(3), 201–207.

Biancini, G. B., Moura, D. J., Manini, P. R., Faverzani, J. L., Netto, C. B., Deon, M., ... Vargas, C. R. (2015). DNA damage in Fabry patients: An investigation of oxidative damage and repair. *Mutation Research Genetic Toxicology and Environmental Mutagenesis*, *784-785*, 31–36.

Blagosklonny, M. V. (2012). Cell cycle arrest is not yet senescence, which is not just cell cycle arrest: Terminology for TOR-driven aging. *Aging*, *4*(3), 159–165.

Campisi, J., & d'Adda, F. F. (2007). Cellular senescence: When bad things happen to good cells. *Nature Reviews Molecular Cell Biology*, *8*(9), 729–740.

Capasso, S., Alessio, N., Squillaro, T., Di Bernardo, G., Melone, M. A., Cipollaro, M., ... Galderisi, U. (2015). Changes in autophagy, proteasome activity and metabolism to determine a specific signature for acute and chronic senescent mesenchymal stromal cells. *Oncotarget*, *6*(37), 39457–39468.

D'Errico, M., Parlanti, E., & Dogliotti, E. (2008). Mechanism of oxidative DNA damage repair and relevance to human pathology. *Mutation Research*, *659*(1-2), 4–14.

De Francesco, P. N., Mucci, J. M., Ceci, R., Fossati, C. A., & Rozenfeld, P. A. (2011). Higher apoptotic state in Fabry disease peripheral blood mononuclear cells: Effect of globotriaosylceramide. *Molecular Genetics and Metabolism*, *104*(3), 319–324.

Debacq-Chainiaux, F., Erusalimsky, J. D., Campisi, J., & Toussaint, O. (2009). Protocols to detect senescence-associated beta-galactosidase (SA-betagal) activity, a biomarker of senescent cells in culture and in vivo. *Nature Protocols*, *4*(12), 1798–1806.

Dominici, M., Le Blanc, K., Mueller, I., Slaper-Cortenbach, I., Marini, F., Krause, D., ... Horwitz, E. (2006). Minimal criteria for defining multipotent mesenchymal stromal cells. The International Society for Cellular Therapy position statement. *Cytotherapy*, *8*(4), 315–317.

Ellaway, C. (2016). Paediatric fabry disease. *Translational Pediatrics*, *5*(1), 37–42.

Fei, X., Jiang, S., Zhang, S., Li, Y., Ge, J., He, B., ... Ruiz, G. (2013). Isolation, culture, and identification of amniotic fluid-derived mesenchymal stem cells. *Cell Biochemistry and Biophysics*, *67*(2), 689–694.

Felsani, A., Mileo, A. M., & Paggi, M. G. (2006). Retinoblastoma family proteins as key targets of the small DNA virus oncoproteins. *Oncogene*, *25*(38), 5277–5285.

Ferraz, M. J., Kallemeijn, W. W., Mirzaian, M., Herrera Moro, D., Marques, A., Wisse, P., ... Aerts, J. M. (2014). Gaucher disease and Fabry disease: New markers and insights in pathophysiology for two distinct glycosphingolipidoses. *Biochimica et Biophysica Acta*, *1841*(5), 811–825.

Fiorentino, F. P., Symonds, C. E., Macaluso, M., & Giordano, A. (2009). Senescence and p130/Rbl2: A new beginning to the end. *Cell Research*, *19*(9), 1044–1051.

Freeman, A. K., & Monteiro, A. N. (2010). Phosphatases in the cellular response to DNA damage. *Cell Communication and Signaling: CCS*, *8*, 27.

Fu, S., Yang, Y., Das, T. K., Yen, Y., Zhou, B. S., Zhou, M. M., ... Kao, J. (2012). Gamma-H2AX kinetics as a novel approach to high content screening for small molecule radiosensitizers. *PLoS ONE*, *7*(6), e38465.

Galderisi, U., Cipollaro, M., & Giordano, A. (2006). The retinoblastoma gene is involved in multiple aspects of stem cell biology. *Oncogene*, *25*(38), 5250–5256.

Galderisi, U., & Giordano, A. (2014). The gap between the physiological and therapeutic roles of mesenchymal stem cells. *Medicinal Research Reviews*, *34*(5), 1100–1126.

Galderisi, U., Helmbold, H., Squillaro, T., Alessio, N., Komm, N., Khadang, B., ... Giordano, A. (2009). In vitro senescence of rat mesenchymal stem cells is accompanied by downregulation of stemness- related and DNA damage repair genes. *Stem Cells and Development*, *18*(7), 1033–1042.

Guenet, J. L. (2011). Animal models of human genetic diseases: Do they need to be faithful to be useful? *Molecular Genetics and Genomics: MGG*, *286*(1), 1–20.

Gullo, F., & De Bari, C. (2013). Prospective purification of a subpopulation of human synovial mesenchymal stem cells with enhanced chondro-osteogenic potency. *Rheumatology*, *52*(10), 1758–1768.

Heidari, B., Shirazi, A., Akhondi, M. M., Hassanpour, H., Behzadi, B., Naderi, M. M., ... Borjian, S. (2013). Comparison of proliferative and multilineage differentiation potential of sheep mesenchymal stem cells derived from bone marrow, liver, and adipose tissue. *Avicenna Journal of Medical Biotechnology*, *5*(2), 104–117.

Helmbold, H., Komm, N., Deppert, W., & Bohn, W. (2009). Rb2/p130 is the dominating pocket protein in the p53-p21 DNA damage response pathway leading to senescence. *Oncogene*, *28*(39), 3456–3467.

Hopkin, R. J., Jefferies, J. L., Laney, D. A., Lawson, V. H., Mauer, M., Taylor, M. R., ... Fabry Pediatric Expert, P. (2016). The management and treatment of children with Fabry disease: A United States-based perspective. *Molecular Genetics and Metabolism*, *117*(2), 104–113.

Kao, J., Milano, M. T., Javaheri, A., Garofalo, M. C., Chmura, S. J., Weichselbaum, R. R., & Kron, S. J. (2006). Gamma-H2AX as a therapeutic target for improving the efficacy of radiation therapy. *Current Cancer Drug Targets*, *6*(3), 197–205.

Kapic, A., Helmbold, H., Reimer, R., Klotzsche, O., Deppert, W., & Bohn, W. (2006). Cooperation between p53 and p130(Rb2) in induction of cellular senescence. *Cell Death and Differentiation*, *13*(2), 324–334.

Lecourt, S., Mouly, E., Freida, D., Cras, A., Ceccaldi, R., Heraoui, D., ... Larghero, J. (2013). A prospective study of bone marrow hematopoietic and mesenchymal stem cells in type 1 Gaucher disease patients. *PLoS ONE*, *8*(7), e69293.

Lee, J. H., & Paull, T. T. (2007). Activation and regulation of ATM kinase activity in response to DNA double-strand breaks. *Oncogene*, *26*(56), 7741–7748.

Leontieva, O. V., & Blagosklonny, M. V. (2010). DNA damaging agents and p53 do not cause senescence in quiescent cells, while consecutive re-activation of mTOR is associated with conversion to senescence. *Aging*, *2*(12), 924–935.

Lieberman, A. P., Puertollano, R., Raben, N., Slaugenhaupt, S., Walkley, S. U., & Ballabio, A. (2012). Autophagy in lysosomal storage disorders. *Autophagy*, *8*(5), 719–730.

Lombard, D. B., Chua, K. F., Mostoslavsky, R., Franco, S., Gostissa, M., & Alt, F. W. (2005). DNA repair, genome stability, and aging. *Cell*, *120*(4), 497–512.

Malafoglia, V., Bryant, B., Raffaeli, W., Giordano, A., & Bellipanni, G. (2013). The zebrafish as a model for nociception studies. *Journal of Cellular Physiology*, *228*(10), 1956–1966.

Mao, Z., Bozzella, M., Seluanov, A., & Gorbunova, V. (2008). DNA repair by nonhomologous end joining and homologous recombination during cell cycle in human cells. *Cell Cycle*, *7*(18), 2902–2906.

Mizushima, N. (2004). Methods for monitoring autophagy. *The International Journal of Biochemistry & Cell Biology*, *36*(12), 2491–2502.

Nagral, A. (2014). Gaucher disease. *Journal of Clinical and Experimental Hepatology*, *4*(1), 37–50.

Najar, M., Raicevic, G., Boufker, H. I., Fayyad Kazan, H., De Bruyn, C., Meuleman, N., . . . Lagneaux, L. (2010). Mesenchymal stromal cells use PGE2 to modulate activation and proliferation of lymphocyte subsets: Combined comparison of adipose tissue, Wharton's Jelly and bone marrow sources. *Cellular Immunology*, *264*(2), 171–179.

Narita, M., Nunez, S., Heard, E., Narita, M., Lin, A. W., Hearn, S. A., . . . Lowe, S. W. (2003). Rb-mediated heterochromatin formation and silencing of E2F target genes during cellular senescence. *Cell*, *113*(6), 703–716.

Oberdoerffer, P., & Sinclair, D. A. (2007). The role of nuclear architecture in genomic instability and ageing. *Nature Reviews Molecular Cell Biology*, *8*(9), 692–702.

Odell, A., Askham, J., Whibley, C., & Hollstein, M. (2010). How to become immortal: Let MEFs count the ways. *Aging*, *2*(3), 160–165.

Ortolano, S., Vieitez, I., Navarro, C., & Spuch, C. (2014). Treatment of lysosomal storage diseases: Recent patents and future strategies. *Recent Patents on Endocrine, Metabolic & Immune Drug Discovery*, *8*(1), 9–25.

Ozcan, S., Alessio, N., Acar, M. B., Mert, E., Omerli, F., Peluso, G., & Galderisi, U. (2016). Unbiased analysis of senescence associated secretory phenotype (SASP) to identify common components following different genotoxic stresses. *Aging*, *8*(7), 1316–1329.

Perry, B. C., Zhou, D., Wu, X., Yang, F. C., Byers, M. A., Chu, T. M., . . . Goebel, W. S. (2008). Collection, cryopreservation, and characterization of human dental pulp-derived mesenchymal stem cells for banking and clinical use. Tissue engineering Part C. *Methods*, *14*(2), 149–156.

Pinnapureddy, A. R., Stayner, C., McEwan, J., Baddeley, O., Forman, J., & Eccles, M. R. (2015). Large animal models of rare genetic disorders: Sheep as phenotypically relevant models of human genetic disease. *Orphanet Journal of Rare Diseases*, *10*, 107.

Platt, F. M., Boland, B., & van der Spoel, A. C. (2012). The cell biology of disease: Lysosomal storage disorders: The cellular impact of lysosomal dysfunction. *The Journal of Cell Biology*, *199*(5), 723–734.

Polo, S. E., & Jackson, S. P. (2011). Dynamics of DNA damage response proteins at DNA breaks: A focus on protein modifications. *Genes & Development*, *25*(5), 409–433.

Prusa, A. R., & Hengstschlager, M. (2002). Amniotic fluid cells and human stem cell research: A new connection. *Medical Science Monitor: International Medical Journal of Experimental and Clinical Research*, *8*(11), RA253–RA257.

Rayess, H., Wang, M. B., & Srivatsan, E. S. (2012). Cellular senescence and tumor suppressor gene p16. *International Journal of Cancer*, *130*(8), 1715–1725.

Roos, W. P., & Kaina, B. (2006). DNA damage-induced cell death by apoptosis. *Trends in Molecular Medicine*, *12*(9), 440–450.

Rufini, A., Tucci, P., Celardo, I., & Melino, G. (2013). Senescence and aging: The critical roles of p53. *Oncogene*, *32*(43), 5129–5143.

Schiffmann, R. (2009). Fabry disease. *Pharmacology & Therapeutics*, *122*(1), 65–77.

Schug, T. T. (2010). MTOR favors senescence over quiescence in p53-arrested cells. *Aging*, *2*(6), 327–328.

Severino, V., Alessio, N., Farina, A., Sandomenico, A., Cipollaro, M., Peluso, G., . . . Chambery, A. (2013). Insulin-like growth factor binding proteins 4 and 7 released by senescent cells promote premature senescence in mesenchymal stem cells. *Cell Death & Disease*, *4*, e911.

Shi, D., & Gu, W. (2012). Dual roles of MDM2 in the regulation of p53: Ubiquitination dependent and ubiquitination independent mechanisms of MDM2 repression of p53 activity. *Genes & Cancer*, *3*(3-4), 240–248.

Shibata, A., Conrad, S., Birraux, J., Geuting, V., Barton, O., Ismail, A., . . . Jeggo, P. A. (2011). Factors determining DNA double-strand break repair pathway choice in G2 phase. *The EMBO Journal*, *30*(6), 1079–1092.

Squillaro, T., Peluso, G., & Galderisi, U. (2016). Clinical trials with mesenchymal stem cells: An update. *Cell Transplantation*, *25*(5), 829–848.

Sun, A., Bagella, L., Tutton, S., Romano, G., & Giordano, A. (2007). From G0 to S phase: A view of the roles played by the retinoblastoma (Rb) family members in the Rb-E2F pathway. *Journal of Cellular Biochemistry*, *102*(6), 1400–1404.

Wei, H., Kim, S. J., Zhang, Z., Tsai, P. C., Wisniewski, K. E., & Mukherjee, A. B. (2008). ER and oxidative stresses are common mediators of apoptosis in both neurodegenerative and non-neurodegenerative lysosomal storage disorders and are alleviated by chemical chaperones. *Human Molecular Genetics*, *17*(4), 469–477.

Xu, S., Cai, Y., & Wei, Y. (2014). MTOR signaling from cellular senescence to organismal aging. *Aging and Disease*, *5*(4), 263–273.

Yoo, S., & Kim, J. B. (2015). Anti-apoptotic and beneficial metabolic activities of resveratrol in type II gaucher disease. *Biological & Pharmaceutical Bulletin*, *38*(6), 913–918.

Zilfou, J. T., & Lowe, S. W. (2009). Tumor suppressive functions of p53. *Cold Spring Harbor Perspectives in Biology*, *1*(5), a001883.

Zion, Y. C., Pappadopulos, E., Wajnrajch, M., & Rosenbaum, H. (2016). Rethinking fatigue in Gaucher disease. *Orphanet Journal of Rare Diseases*, *11*(1), 53.

Zuckerman, V., Wolyniec, K., Sionov, R. V., Haupt, S., & Haupt, Y. (2009). Tumour suppression by p53: The importance of apoptosis and cellular senescence. *The Journal of Pathology*, *219*(1), 3–15.

How to cite this article: Squillaro T, Antonucci I, Alessio N, et al. Impact of lysosomal storage disorders on biology of mesenchymal stem cells: Evidences from in vitro silencing of glucocerebrosidase (GBA) and alpha-galactosidase A (GLA) enzymes. *J Cell Physiol*. 2017;9999:1–14. https://doi.org/10.1002/jcp.25807